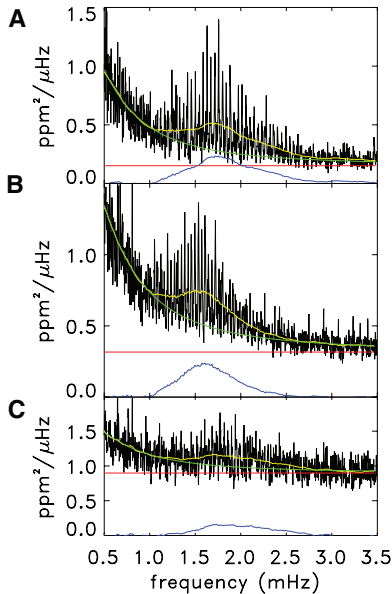
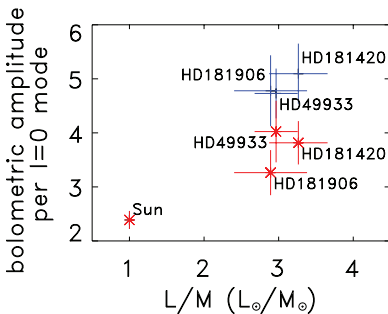


24 OCTOBER 2008 VOL 322 **SCIENCE** www.sciencemag.org

Table 1. Parameters obtained in the present analysis, with standard deviation estimates.

Star	A_{bol} ($l = 0$)(ppm)	B_{bol} (ppm ² /μHz)	C (s)	Δ (μHz)
HD 49933	4.02 ± 0.57	1.97 ± 0.53	1967 ± 431	86 ± 2
HD 181420	3.82 ± 0.40	2.41 ± 0.31	1936 ± 206	77 ± 2
HD 181906	3.26 ± 0.42	1.12 ± 0.20	1650 ± 0276	88 ± 2
Sun PMO6	2.39 ± 0.17	0.85 ± 0.06	1440 ± 86	135 ± 2

**Fig. 2.** Instrumental power spectral density. (A) For HD49933; a moving mean is applied with a 4-μHz boxcar (black); yellow curve: same spectrum highly smoothed (4 times Δ boxcar); green curve: mean level of the granulation + white noise components; red curve: mean white noise component level alone; blue curve: oscillation mean power density contribution alone. (B) Same for HD181420. (C) Same for HD181906.**Fig. 3.** Maximum bolometric amplitudes per radial mode measured (red) for HD49933, HD181420, HD181906, and for the Sun. Theoretical values are also given (blue). Error bars on amplitudes are standard deviation estimates associated with the accuracy of the measurements (red), and with the error estimate on T_{eff} (blue).

Stellaires) (9)]. For alpha Cen A, WIRE (10) detected the characteristic comblike pattern of the oscillations, which could be analyzed with

the help of complementary velocity data (11). However, alpha Cen A is very close to the Sun in terms of its global characteristics. The results here are based on light curves obtained with CoRoT over 60 days for HD49933 and 156 days for HD181420 and HD181906, three main sequence F stars noticeably hotter than the Sun (Fig. 1 and table S1).

The CoRoT satellite was launched on December 2006 in an inertial polar orbit at an altitude of 897 km. The instrument is fed by a 27-cm diameter telescope. During each run, it simultaneously provides light curves (variations in stellar flux with time) from 10 bright stars ($5.5 < m_V < 9.5$) dedicated to seismic studies, while 12,000 fainter stars ($11.5 < m_V < 15.5$) are monitored to search for transits due to planets (6). The sampling rate is 1 s for an integration time of 0.794 s. Pointing stability reaches a precision of 0.15" root mean square. The duty cycle was higher than 93%; the missing data correspond essentially to the time spent in the South Atlantic magnetic anomaly where the perturbations due to energetic particles have not, as yet, been effectively corrected. These gaps, about eight per day, from 5 to 15 min each, have been linearly interpolated (with a 2000-s boxcar on each side of the gap to prevent the introduction of any spurious high frequencies) before we computed the Fourier power spectra, to minimize the aliases of the low-frequency components due to the window. We used synthetic spectra to check that this procedure has no noticeable influence on the measured mean values.

For each of the three stars, the Fourier power density spectra (Fig. 2) show three components that can be understood as (i) a flat white-noise component essentially due to photon counting noise, (ii) a stellar background component (essentially granulation in this frequency domain) following a Lorentzian profile $B/[1+(C\nu)^2]$ as suggested in (12), and (iii) the stellar oscillation spectrum with its comblike pattern characterized by the large separation Δ (13).

Although dedicated analyses are under way to extract individual mode frequencies and profiles for each star, we measure here the contributions of these three components. We follow the method proposed in (14) and illustrated in Fig. 2, and we convert these instrumental values into intrinsic bolometric maximum amplitude per radial mode [$A_{\text{bol}}(l = 0)$] and bolometric maximum power spectral density B_{bol} (15). We apply the same analysis to the solar SOHO/VIRGO/PMO6 (Solar and Heliospheric Observatory/

Variability of Solar Irradiance and Gravity Oscillations) data (16). The amplitudes of the three stars are larger than in the Sun by a factor of ~ 1.5 (Fig. 3).

Theoretical predictions suggest that velocity amplitudes follow a scaling law in $(L/M)^\alpha$ with $\alpha \sim 0.7$ (L and M standing for luminosity and mass), in broad agreement with the existing velocity measurements (17). In the adiabatic approximation (18), this would give photometric amplitudes scaling as $(L/M)^\alpha (T_{\text{eff}})^{1/2}$, where T_{eff} is effective temperature. As shown in Fig. 3 (see also Table 1), the measured values for the three stars are of the same order but significantly lower (by $24 \pm 8\%$ globally) than the theoretical values. The measurement of this systematic departure from the adiabatic case, which is not observed in velocity, tells us about the exchange of energy between convection and oscillations in the outer part of the convection zone. This process is responsible for the existence, and the specific amplitudes and lifetimes, of the oscillations. Both radial velocity and photometry measurements are sensitive to the oscillation momentum induced by this energy exchange; the photometric amplitudes are in addition more sensitive to the details of this process, via radiation-matter interaction. These measurements offer the possibility of testing theoretical models of the nonadiabatic effects of the processes governing the oscillations and illustrate the complementary interest of photometry and radial velocity measurements (when they are possible), which probe the oscillations differently.

The spectral signature of granulation is expected to reveal time scales and distance scales characteristic of the convection process in different stars (12, 19). Our data show (fig. S1 and Table 1) that (i) the maximum bolometric power density (B_{bol}), associated with the number of eddies seen at the stellar surface and the border/center contrast of the granules, is higher for the three stars than for the Sun by a factor up to 3; and (ii) the characteristic time scale for granulation (C) associated with the eddy turnover time increases slightly with T_{eff} (up to 30% higher than the Sun).

References and Notes

1. A. Claverie, G. R. Isaak, C. P. McLeod, H. B. van der Raay, T. Roca Cortes, *Nature* **282**, 591 (1979).
2. G. Grec, E. Fosfat, M. Pomerantz, *Nature* **288**, 541 (1980).
3. D. Gough, J. W. Leibacher, P. Scherrer, J. Toomre, *Science* **272**, 1281 (1996).
4. J. M. Matthews et al., *Nature* **430**, 51 (2004).
5. D. G. Guenther et al., *Astrophys. J.* **635**, 547 (2005).
6. A. Baglin et al., in *The CoRoT Mission, Pre-Launch Status, Stellar Seismology and Planet Finding*, M. Fridlund, A. Baglin, J. Lochard, L. Conroy, Eds. (ESA SP-1306, ESA Publications Division, Noordwijk, Netherlands, 2006), pp. 33–37.
7. H. Bruntt et al., *Astrophys. J.* **633**, 440 (2005).
8. C. Karoff, H. Bruntt, H. Kjeldsen, T. Bedding, D. L. Buzasi, *Commun. Asteroseismol.* **150**, 147 (2007).
9. D. B. Guenther et al., *Commun. Asteroseismol.* **151**, 5 (2007).
10. J. Schou, D. L. Buzasi, in *Proceedings SOHO 10/GONG 2000 Workshop: Helio- and Asteroseismology at the Dawn of the Millennium*, P. L. Pallé, A. Wilson, Eds. (ESA SP-464, ESA Publications Division, Noordwijk, Netherlands, 2001), pp. 391–394.

11. S. T. Fletcher, W. J. Chaplin, Y. Elsworth, J. Schou, D. Buzasi, in *Proceedings SOHO 18/GONG 2006/HELAS I, Beyond the Spherical Sun*, K. Fletcher, M. Thompson, Eds. (ESA SP-624, ESA Publications Division, Noordwijk, Netherlands, 2006), published on CDROM, p. 27.1.
12. J. W. Harvey, *Proceedings Future Missions in Solar, Heliospheric and Space Plasma Physics*, E. Rolfe, B. Battrock, Eds. (ESA-SP 235, ESA Publications Division, Noordwijk, Netherlands, 1985), pp. 199–208.
13. The large separation (Δ) refers to the first order regular spacing in frequency between consecutive overtone eigenfrequencies, responsible for the characteristic comb-like pattern of the oscillation spectrum.
14. H. Kjeldsen *et al.*, *Astrophys. J.* **635**, 1281 (2005).
15. Materials and methods are available as supporting material on Science Online.
16. C. Frohlich *et al.*, *Sol. Phys.* **170**, 1 (1997).
17. R. Samadi *et al.*, *Astron. Astrophys.* **463**, 297 (2007).
18. H. Kjeldsen, T. R. Bedding, *Astron. Astrophys.* **293**, 87 (1995).
19. F. Baudin, R. Samadi, T. Appourchaux, E. Michel, in *The CoRoT Mission, Pre-Launch Status, Stellar Seismology and Planet Finding*, M. Fridlund, A. Baglin, J. Lochard, L. Conroy, Eds. (ESA SP-1306, ESA Publications Division, Noordwijk, Netherlands, 2006), pp. 403–407.
20. Y. Lebreton, E. Michel, *Astrophys. Space Sci.* **316**, 167 (2008).
21. The CoRoT space mission, launched on December 2006, was developed and is operated by CNES (Centre National d'Etudes Spatiales), with participation of the Science

Program of ESA, ESA's RSSD (Research and Scientific Support Department), Austria, Belgium, Brazil, Germany, and Spain. We acknowledge the access to data from the VIRGO instrument aboard SOHO, the mission of international collaboration between ESA and NASA.

Supporting Online Material

www.sciencemag.org/cgi/content/full/322/5901/558/DC1

SOM Text

Fig. S1

Table S1

References

9 July 2008; accepted 10 September 2008

10.1126/science.1163004

A Large Excess in Apparent Solar Oblateness Due to Surface Magnetism

Martin D. Fivian,^{1*} Hugh S. Hudson,¹ Robert P. Lin,^{1,2} H. Jabran Zahid^{1,3}

The shape of the Sun subtly reflects its rotation and internal flows. The surface rotation rate, ~ 2 kilometers per second at the equator, predicts an oblateness (equator-pole radius difference) of 7.8 milli-arc seconds, or $\sim 0.001\%$. Observations from the Reuven Ramaty High-Energy Solar Spectroscopic Imager satellite show unexpectedly large flattening, relative to the expectation from surface rotation. This excess is dominated by the quadrupole term and gives a total oblateness of 10.77 ± 0.44 milli-arc seconds. The position of the limb correlates with a sensitive extreme ultraviolet proxy, the 284 angstrom limb brightness. We relate the larger radius values to magnetic elements in the enhanced network and use the correlation to correct for it as a systematic error term in the oblateness measurement. The corrected oblateness of the nonmagnetic Sun is 8.01 ± 0.14 milli-arc seconds, which is near the value expected from rotation.

Motions within the interior of the Sun affect the location of the photosphere, so the precise measurement of the shape of the solar limb is a long-standing astrometric objective (1). The shape also relates to Le Verrier's 1859 observation of an anomalous perihelion precession of Mercury (only some 43" per century), which could be precisely cal-

culated in Einstein's theory of general relativity (2). A discrepancy from the predictions of this theory would point to either a need for a new theory or else to a distortion of the Sun's internal gravity not reflected in the surface rotation. The two leading possibilities for such a gravitational field would be a rapidly rotating core left over from the early stages of star

formation—perhaps on an oblique axis—or a strong magnetic field (3).

The modern era of measurements of the solar oblateness began in the 1960s with Dicke's Princeton Solar Distortion Telescope (4) and other ground-based telescopes (5–8). Dicke's initial results (4) implied that the Sun was much more oblate than the surface rotation predicts. More recent observations have tended to show smaller values, closer to the 7.8 milli-arc sec predicted by the surface rotation (3), but the uncertainties in the measurements have remained relatively large. The theoretical estimate is difficult because of the differential nature of solar rotation, both in latitude and in radius. The ground-based data also hinted at time variations in the oblateness (6). Including the two data points (1997 and 2001) from the Michelson-Doppler Imager (9) on board the Solar Heliospheric Ob-

¹Space Sciences Laboratory, University of California–Berkeley, Berkeley, CA 94720, USA. ²Physics Department, University of California–Berkeley, Berkeley, CA 94720, USA. ³Institute for Astronomy, University of Hawaii, Manoa, HI 96822, USA.

*To whom correspondence should be addressed. E-mail: mfivian@ssl.berkeley.edu

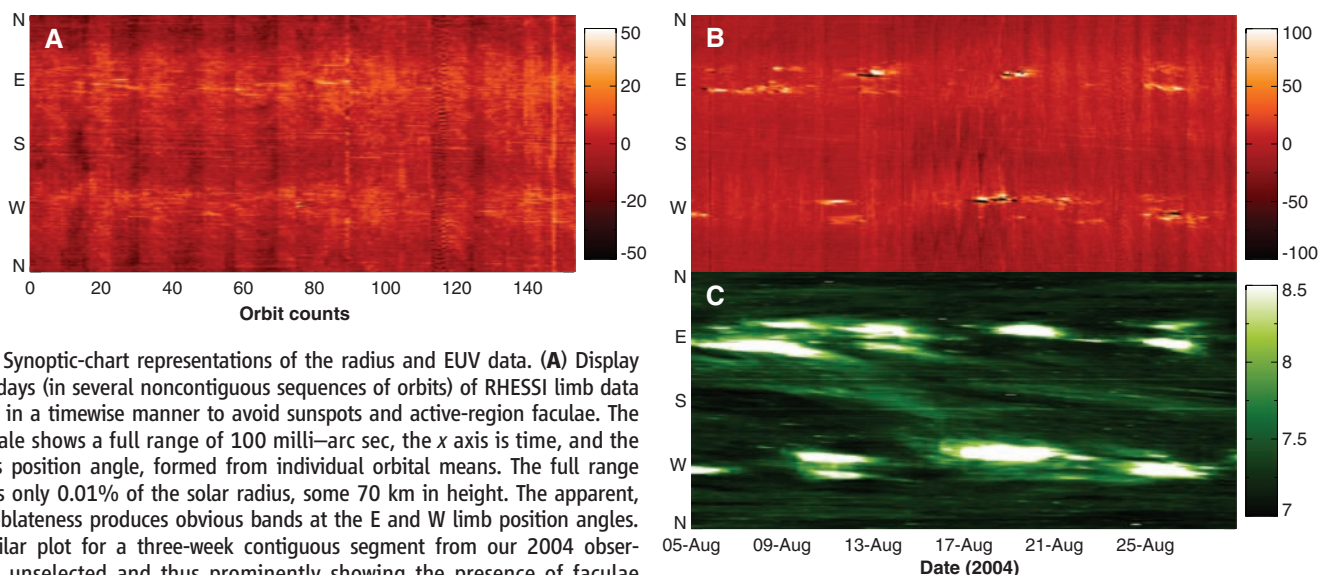


Fig. 1. Synoptic-chart representations of the radius and EUV data. (A) Display of ~ 10 days (in several noncontiguous sequences of orbits) of RHESSI limb data selected in a timewise manner to avoid sunspots and active-region faculae. The color scale shows a full range of 100 milli-arc sec, the x axis is time, and the y axis is position angle, formed from individual orbital means. The full range shown is only 0.01% of the solar radius, some 70 km in height. The apparent, excess oblateness produces obvious bands at the E and W limb position angles. (B) Similar plot for a three-week contiguous segment from our 2004 observations, unselected and thus prominently showing the presence of faculae (bright) and sunspots (dark). (C) Corresponding limb data from the SOHO observations in the EUV 284 Å band (18), which shows the locations of faculae and other kinds of magnetic activity. The contours of this synoptic map determine the data fraction for our masking analysis, as detailed in the SOM.